

Article

Continental Arc Flare-Ups and Crustal Thickening Events in NE China: Insights from Detrital Zircon U-Pb Dating and Trace Elements from the Heilongjiang Complex

Yanchen Pan ¹, Mengyu Xu ², Kai Liu ^{3,*} and Meng Wang ⁴¹ School of Water Resources and Environment, China University of Geosciences, Beijing 100083, China² Institute of Geology and Geophysics, Chinese Academy of Sciences, Beijing 100029, China³ School of Earth Sciences and Resources, China University of Geosciences, Beijing 100083, China⁴ Key Laboratory of Western Mineral Resources and Geological Engineering, MOE, School of Earth Science and Resources, Chang'an University, Xi'an 710054, China; wangmeng@chd.edu.cn

* Correspondence: k.liu@cugb.edu.cn

Abstract: Continental arc is characterized by alternant magmatic flare-ups and lulls. From the Permian to the Middle Jurassic period, two flare-ups with a lull developed in NE China, but the tectonic controls that caused the flare-ups remain unclear. Sedimentary rocks of the Heilongjiang Complex were derived from these magmatic rocks; thus, we employed detrital zircon U-Pb dating and trace elements analyses to unravel the regional tectono-magmatic evolution. Eu anomaly, $(Dy/Yb)_N$ and Th/U ratios of the detrital zircons and Sr/Y and $(La/Yb)_N$ of the regional granitoids together indicate the occurrence of two episodes of crustal thickening during the two flare-ups, accompanied with a westward migration of magmatism. We propose that the Permian flare-up was caused by the shallowing subduction from the east, which thickened the upper plate and enhanced the deep crustal melting. During the Middle Triassic period, the mantle wedge was expelled by the flat slab and thickened crust, leading to the magmatic lull. However, the westward subduction of the back-arc oceanic plate occurred before the lull, gradually producing the Jurassic magmatic flare-up and crustal thickening. Closure of the back-arc ocean caused by the outboard Paleo-Pacific oceanic plate subduction was important in the formation of the episodic magmatic flare-ups and crustal thickening in NE China.

Keywords: continental arc; arc magma tempo; detrital zircon; accretionary orogen



Citation: Pan, Y.; Xu, M.; Liu, K.; Wang, M. Continental Arc Flare-Ups and Crustal Thickening Events in NE China: Insights from Detrital Zircon U-Pb Dating and Trace Elements from the Heilongjiang Complex. *Minerals* **2023**, *13*, 1121. <https://doi.org/10.3390/min13091121>

Academic Editors: Jiafu Chen, Nan Ju, Zhonghai Zhao and Petrus J Le Roux

Received: 17 July 2023

Revised: 19 August 2023

Accepted: 23 August 2023

Published: 25 August 2023



Copyright: © 2023 by the authors. Licensee MDPI, Basel, Switzerland. This article is an open access article distributed under the terms and conditions of the Creative Commons Attribution (CC BY) license (<https://creativecommons.org/licenses/by/4.0/>).

1. Introduction

Continental arc shows periodicity. Although a continental arc have persisted for hundreds of millions of years, its flux significantly varied and showed alternate magmatic flare-ups ($70\text{--}90\text{ km}^3\text{ km}^{-1}\text{ Myr}^{-1}$) and lulls ($<20\text{ km}^3\text{ km}^{-1}\text{ Myr}^{-1}$) [1]. Each flare-up or lull lasted for several tens of millions of years, consisting of the “continental arc tempo” [2]. However, which tectonic process triggered this tempo remains unclear and this limits our understanding of the continental arc magmatism. Because arc magmatism and differentiation were the key to generate continental crust, unravelling the arc tempo will directly help to understand how the continent was formed and evolved [3].

The orogenic cyclicity, or periodicity was defined along the eastern Pacific margin, the American Cordillera [3]. Taking Sierra Nevada as an example, although continental arc magmatism was first initiated in the early Mesozoic era, there were only two main flare-ups, occurring in the Middle to Late Jurassic and the mid-Cretaceous periods, respectively [4]. It was noted that the two flare-ups were closely associated with strong regional compression, crustal thickening, and landward migration of arc magmatism. Based on the data from both the North and South American Cordillera, Decellas et al. (2009) suggested that these aforementioned associations were widespread in the Andes, Sierra Nevada, Canada Coastal

Mountains, and other parts of the American Cordilleran belt; after the landward migration of the arc magmas, they waned and migrated back toward the trench before the next round of flare-up, crustal thickening, and landward migration [3]. Ducea (2001) pointed out a key factor in this orogenic cyclicity, that is, each magmatic flare-up corresponded to more evolved Nd isotopic features (isotope “pull-down”) [5]. Therefore, it is indicated that increasing magmatic flux was somehow related to the involvement of enriched, mature continental materials.

Although many tectonic models were proposed, controversies exist in many aspects [1]. First, some studies suggested that the landward arc migration was caused by slab angle shallowing [6], but some others believed that crustal thickening with magmatic addition and regional compression could migrate the arc without slab shallowing [7]. Second, why did the magmas show enriched isotopes during flare-ups? An early explanation was that the isotopes formed due to the “under-thrusting” of the rear-arc continental crust deep into the arc source, which supplied fertile and mature materials to the magmas [3,5]. Recent research proposed that the arc magmas were more enriched simply because they moved to the ancient continental interior and the addition of rear-arc materials was not necessary [8]. Some studies even suggested that it was the mantle input that triggered the magmatic flare-ups based on the juvenile zircon Hf isotopes [9]. Third, which tectonic mechanism drive the cyclicity? Many studies indicate that the crustal thickening transformed the lower continental arc crust to eclogites, and they finally foundered into the mantle, thereby thinning the crust [3,4]. Afterwards, regional compression thickened the crust again and the orogen evolved to the next cycle. According to this viewpoint, cyclicity is self-driven, influenced only by the internal factors of the orogen matter. However, other studies have suggested that external factors dominate the orogeny, such as the change in slab angle, subduction rate, and so on [1,6].

During the Early Permian to Middle Jurassic, N-S trending calc-alkaline magmatic belts developed in NE China (Figure 1), representing long-lived continental arc activities [10–13]. These arc magmas also show typical landward migration trends [11,14], similar to the situations in the American Cordillera, providing us with an opportunity to test the contested views regarding the orogenic cyclicity. However, some important geological parameters, such as crustal thickness, have been largely changed due to the surface processes for >150 Myr; most geological records were also superposed or changed due to the tectonic activities, especially the multiple episodes of regional compression, shearing, and extension.

The Heilongjiang Complex is a Mesozoic accretionary complex in NE China and represents the remnants of the Mudanjiang Ocean [15], a fossil oceanic basin between the Jiamusi and Songliao blocks, with sedimentary materials deposits mainly from the nearby continental arc magmatic rocks [13]. Recently, trace elements with coupled U-Pb ages of detrital zircons become a useful tool to indicate the tectonic evolution of continental arcs [16]. This is because many volcanic rocks and shallow plutonic rocks have been eroded, and many parts of a now-exhumed arc are covered with sediments or vegetations, making them inaccessible for sampling. But zircons could survive both surface erosion and several rounds of recycling low- to middle-grade (hydro-)thermal alteration.

In this study, we employed U-Pb dating and trace elements analyses of detrital zircons from the Heilongjiang Complex, integrated with published data from regional magmatic rocks and detrital zircons, in order to explore the evolution of continental arcs in NE China. We propose a tectonic model to explain the continental arc tempos in NE China and compare the geodynamic mechanism with the American Cordillera.

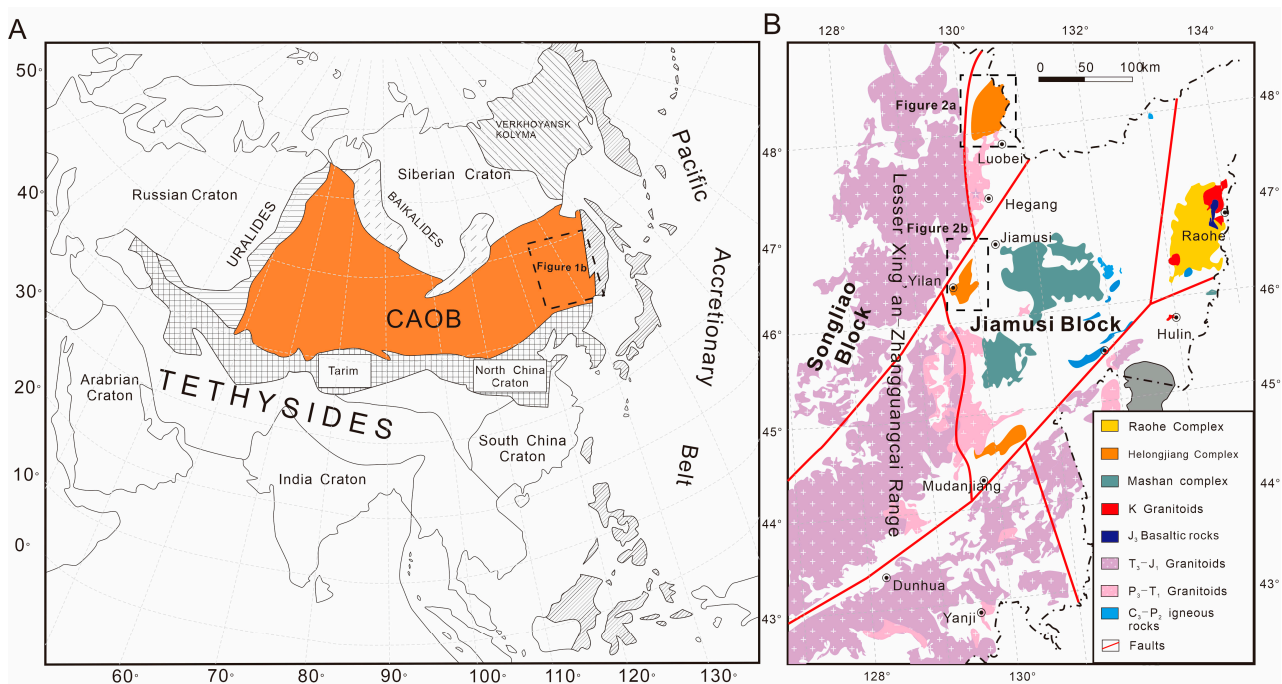


Figure 1. (A) Tectonic position of the study area (after [17]); (B) simplified geological map of the eastern Heilongjiang Province (after [14]). Our samples were collected from the Heilongjiang Complex, near Luobei and Yilan.

2. Geological Setting and Sampling

The study area is located in NE China, east of the Songliao Basin, tectonically including the eastern Songliao and Jiamusi blocks (Figure 1B).

The Songliao Block include the Lesser Xing'an-Zhangguangcai Range along the eastern margin, and most other parts are covered by the post-Cretaceous strata in the Songliao Basin. Previous studies suggested that the basement of the Songliao Basin is juvenile crust and mainly contains the Paleozoic to Mesozoic meta-volcanic, meta-sedimentary rocks, and granitic gneisses. However, recent studies reported ages of ca. 1.8 Ga from meta-gabbros and meta-granitic breccias from the drill holes [18]. From the Middle Jurassic, the Songliao Basin experienced initial rifting, post-rifting subsidence, and basin inversions [19,20]. The most important volcanism in the basin occurred in the Early Cretaceous (c. 135–100 Ma) [12,21]. The Lesser Xing'an-Zhangguangcai Range is located along the eastern Songliao Block (Figure 1B), and mainly consisted of granitoids with various ages [10,22], including the Early Paleozoic (c. 510–470 Ma), Early Permian (280–290 Ma), Late Permian to Early Triassic (c. 260–240 Ma), Late Triassic to Early Jurassic (220–170 Ma), and middle Cretaceous (c. 100 Ma). The most widespread magmatic episode occurred in the Late Triassic to Early Jurassic [22].

The Bureya-Jiamusi-Khanka Block is cut by the north branches of the Tan-Lu Fault, namely the Dunhua-Mishan and Jiamusi-Yilan faults (Figure 1B); the Jiamusi Block is the central part bounded by the two faults. (Figure 1B). The oldest rocks in the Jiamusi Block have ages ranging from c. 891 to 898 Ma [23]; an almost similar age (c. 933 Ma) is reported in the Bureya Block as well [24]. Thus, the Neoproterozoic could be the basement age of this united continental block. However, the most important basement of the block was formed during the late Pan-African period (c. 500 Ma) [17,25], including granulite-facies metasedimentary and minor meta-mafic rocks, accompanied by the Early Paleozoic granitoids [25]. Along the eastern Jiamusi and Khanka blocks, there are some Paleozoic volcanic and sedimentary strata. The main lithologies are the Early Paleozoic marbles, terrigenous clastic rocks, and the Late Paleozoic volcanic rocks with intervening terrigenous clastic rocks. Calc-alkaline arc-like andesites and dacites firstly occurred in the Early

Permian, indicating the early-stage continental arc in the region [26]. From the Early Permian to the earliest Triassic, N-S trending granitoids with associated volcanic rocks were generated and migrated throughout the whole block from east to west, mainly consisting of calc-alkaline granitoids [11]. However, there are very few magmatic records from the late Early Triassic to Jurassic in the Jiamusi block, although these ages have been reported along the western Bureya and Khanka blocks [27]. Volcanic rocks with minor plutonic rocks increased in the Early Cretaceous and are most abundant from the late Early to early Late Cretaceous in the Jiamusi block, and mainly show intra-plate affinities [12,22].

There are several fragments of Mesozoic accretionary complexes along the western margin of the Jiamusi block (Figure 1B), which are named as the Heilongjiang Complex, representing a lost ocean (the Mudanjiang Ocean) between the Songliao and Jiamusi blocks [15]. The Heilongjiang Complex is composed of mica schist, marble, quartzite, greenschist, blueschist, and amphibolite. Most published data show that the protolith age of the blueschist is Early Permian to Triassic (c. 285 to 213 Ma), whereas the high-pressure metamorphic age ranges from c. 210 to 170 Ma [15]. However, a blueschist sample from Yilan yields a concordant zircon U-Pb age of 142 Ma, which is the only Cretaceous protolith age of rocks from the Heilongjiang Complex so far [28]. There are also some other accretionary complexes exposed in the region, such as the N-S trending Zhangguangcai Complex along the eastern Songliao block [29]. It consists of amphibolite, biotite-plagioclase-gneiss, marble, schist, and meta-volcanic rocks. The metamorphic ages range from the Paleozoic to the Early Mesozoic [29].

Eight meta-sedimentary rock samples were collected from the two areas of the Heilongjiang Complex, near Luobei and Yilan, respectively (Figures 1B and 2). These samples are exposed as strongly deformed matrix (Figures 3 and 4), within which metamorphic basaltic rocks (such as greenschist) were observed and they are commonly intruded by later-stage magmatic rocks (Figure 3). Details of the samples are listed in Table 1, including the sample numbers, GPS locations, and lithologies.

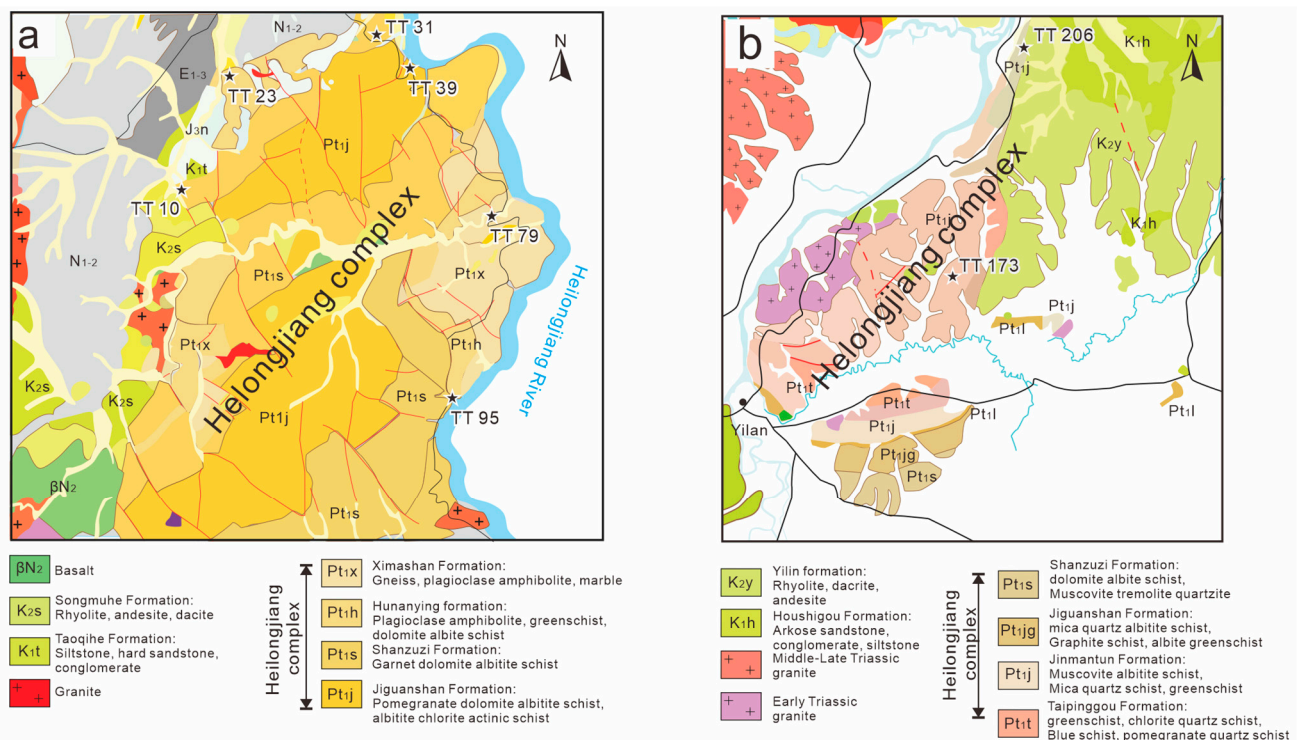


Figure 2. Geological maps of the sampling locations (after local 1:200,000 geological map). See Table 1 for details of the samples. (a) Map of the Jiayin-Luobei area and (b) the Jiamusi-Yilan area.

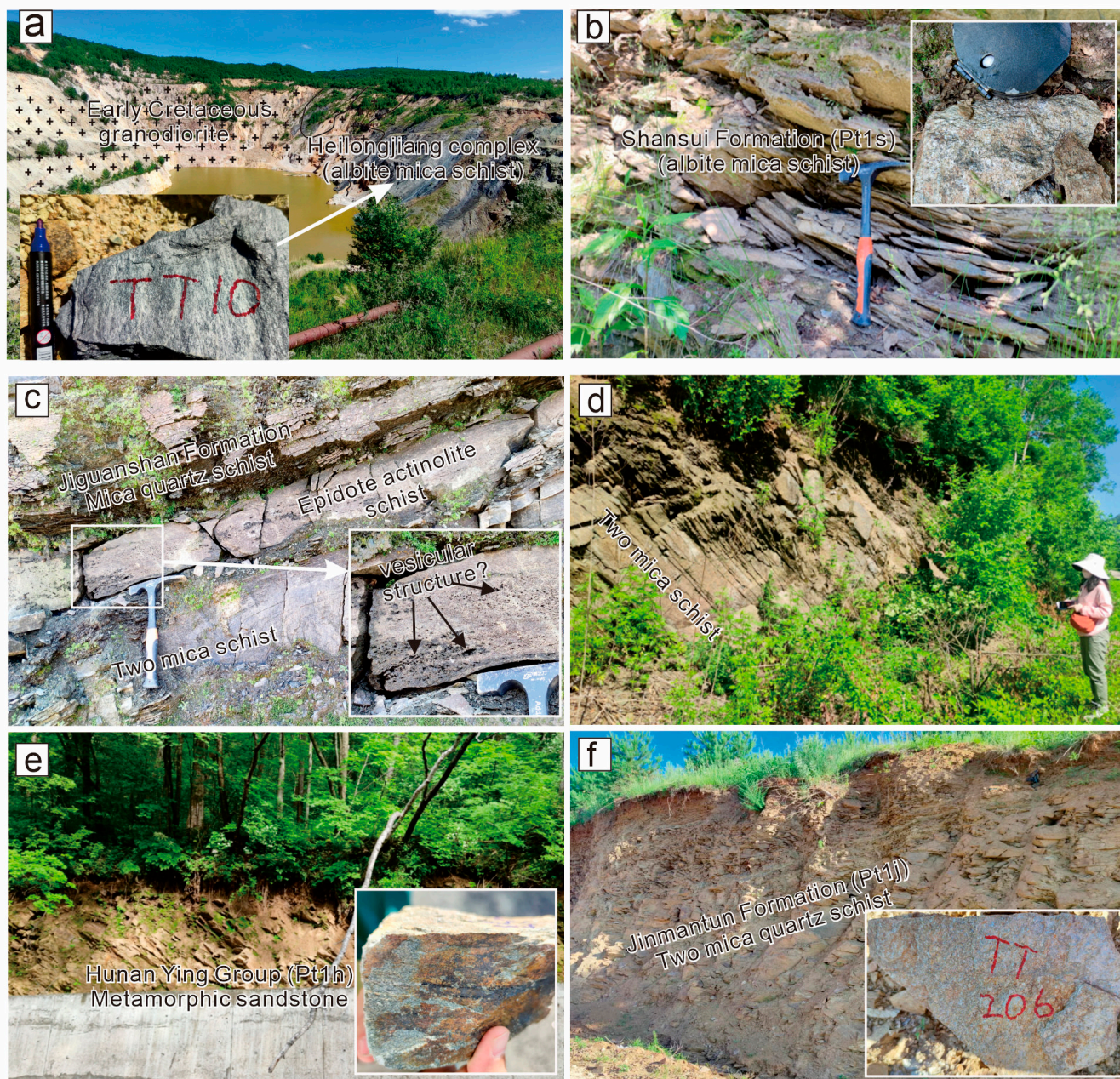


Figure 3. Typical outcrops of the sampling locations. (a) Gold mine near Wulaga, with the Early Cretaceous granodiorite intruding into the Heilongjiang Complex; (b) the Shanzuizi Group (albite mica schist) in Jiayin; (c) the Jiguanshan Group (two mica schist) near the mouth of the Jiayin river and there are residual vesicles in the greenschist layer; (d,e) show mica schist and meta-sandstone to the north of Luobei; (f) the Jinmantun Group (two mica quartz schist) near Jiamusi.

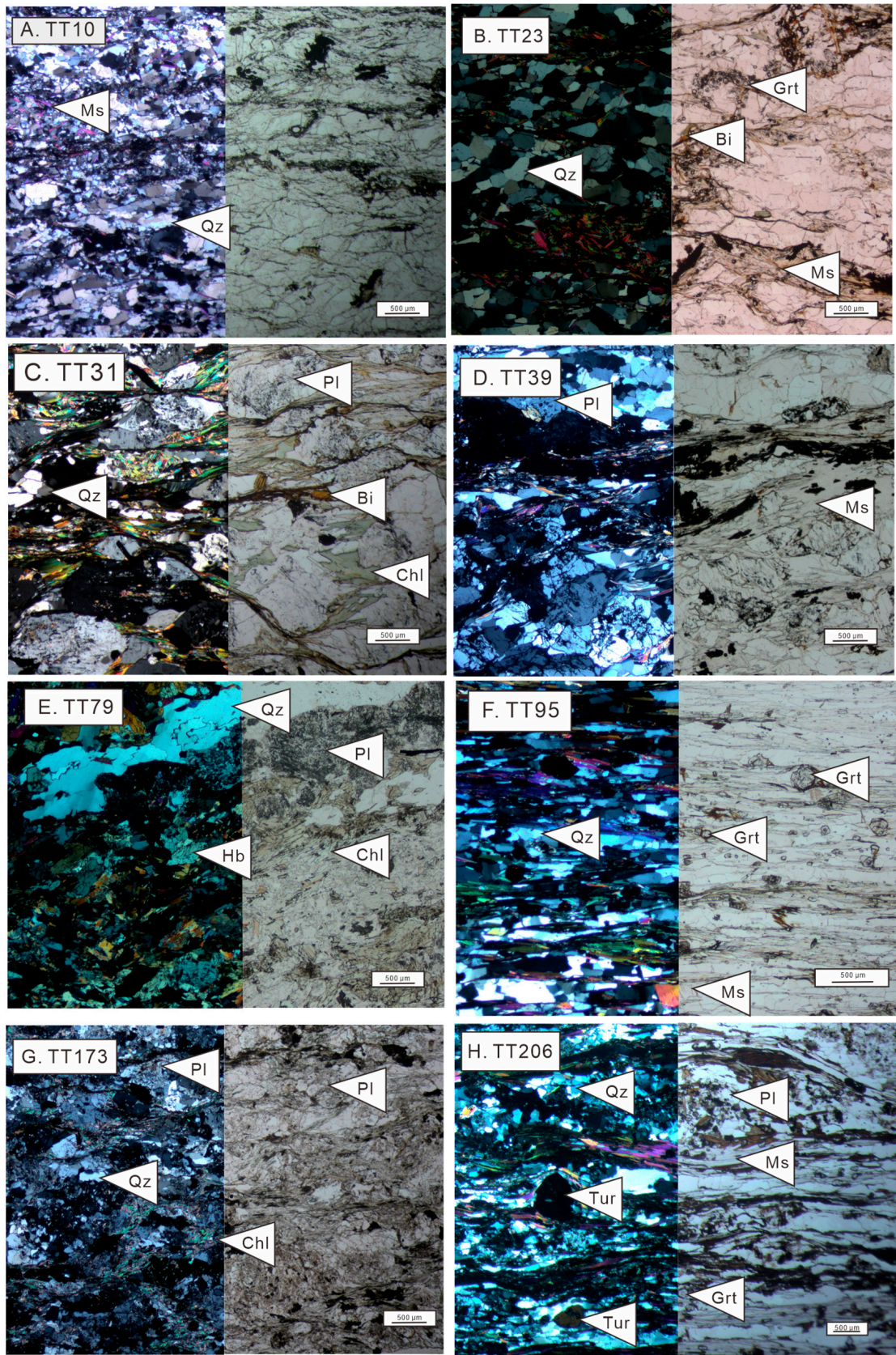


Figure 4. Thin sections of the 8 meta-sedimentary rocks in this study.

Table 1. Sample information of meta-sedimentary rocks from the Heilongjiang Complex.

Sample Number	GPS Location	Area	Descriptions
TT10	E 130°15'2.9" N 48°22'34.4"	Jiayin-Luobei	Grey, mica schist; Qz (>85%) + muscovite mica (5%–10%) + opaque mineral (3%–5%).
TT23	E 130°19'18.6" N 48°28'29.9"		Grey, garnet two-mica quartz schist; Qz (65%) + muscovite mica (15%) + biotite (5%) + opaque mineral (3%); accessory minerals: garnet, chlorite.
TT31	E 130°33'14.9" N 48°30'44.8"		Grey greenish, biotite greenschist; highly deformed; Plagioclase (55%) + Qz (15%) + chlorite (25%) + biotite (5%).
TT39	E 130°36'35" N 48°28'46.4"		Grey, mica schist; Plagioclase (35%) + Qz (35%) + muscovite mica (25%) + opaque mineral (5%).
TT79	E 130°44'15.6" N 48°19'58.3"		Dark grey, hornblende greenschist; deformed; Plagioclase (55%) + chlorite (20%) + hornblende (15%) + Qz (10%).
TT95	E 130°40'0.7" N 48°09'6.5"		Yellowish, garnet mica schist; highly deformed; Qz (75%) + muscovite mica (20%) + garnet (5%).
TT173	E 129°52'23.7" N 46°27'8"	Yilan-Jiamusi	Dark grey, quartz greenschist; highly deformed; Plagioclase (70%) + Qz (15%) + chlorite (15%).
TT206	E 129°58'4.59" N 46°40'14.32"		Light grey, garnet muscovite mica schist; highly deformed; plagioclase (40%) + Qz (35%) + muscovite mica (20%) + tourmaline (3%) + garnet (2%).

We first selected detrital zircons from these samples, and then carried out U-Pb dating and trace elements analyses. See the Table S1 for details of the results, Table S2 for the compiled whole-rock geochemical data, and Table S3 for the methods used in this study. According to the temporal variations of zircon geochemical features, combined with the geochemical and geochronological data from the regional magmatic rocks, we discuss the tectonic evolution of the two episodes of continental arc in NE China.

3. Results

Most zircons from our eight samples show inherited cores with oscillatory zonation, indicating their magmatic origins (Figure 5). The internal zonation patterns in the cores differ from each other, e.g., some zoning intervals are wide and some others are narrow (Figure 5). This is because they are detrital zircons which were derived from various source rocks with different magmatic evolution history. However, almost all the grains are characterized by very thin bright rims in the cathode luminescence (CL) images. The rims have irregular boundaries with the magmatic zircon cores (Figure 5), probably caused by fluid-assisted hydrothermal alteration in low temperature metamorphism [30].

Nightly concordant ages yielded in sample TT10 (Figure 6a), ranging from 165 to 527 Ma. Zircons have length/width ratios varying from 1:1 to 4:1, and the lengths range from 80 to 200 μm (Figure 4). The age groups are divided into four categories: 509–527 Ma (2.2%), 436–458 Ma (3.3%), 216–269 Ma (12.1%), and 165–206 Ma (82.4%). The final group constitutes the major age peak (c. 182 Ma) in this sample, whereas the other three groups show very weak peak ages at 253 Ma, 455 Ma, and 509 Ma, respectively. According to the youngest age at c. 165 Ma and the youngest peak age at c. 182 Ma, the maximum depositional age of sample TT10 is the Middle Jurassic.

Zircons from sample TT23 show similar sizes and shapes to those from sample TT10. Nineteen-eight concordant results were obtained (Figure 6b), ranging from 153 Ma to 1874 Ma. More than 90% zircons have ages from 153 to 241 Ma, showing a major peak at c. 176 Ma. The maximum depositional age of sample TT23 should be the Middle Jurassic, based on the youngest zircon grain age at c. 153 Ma.

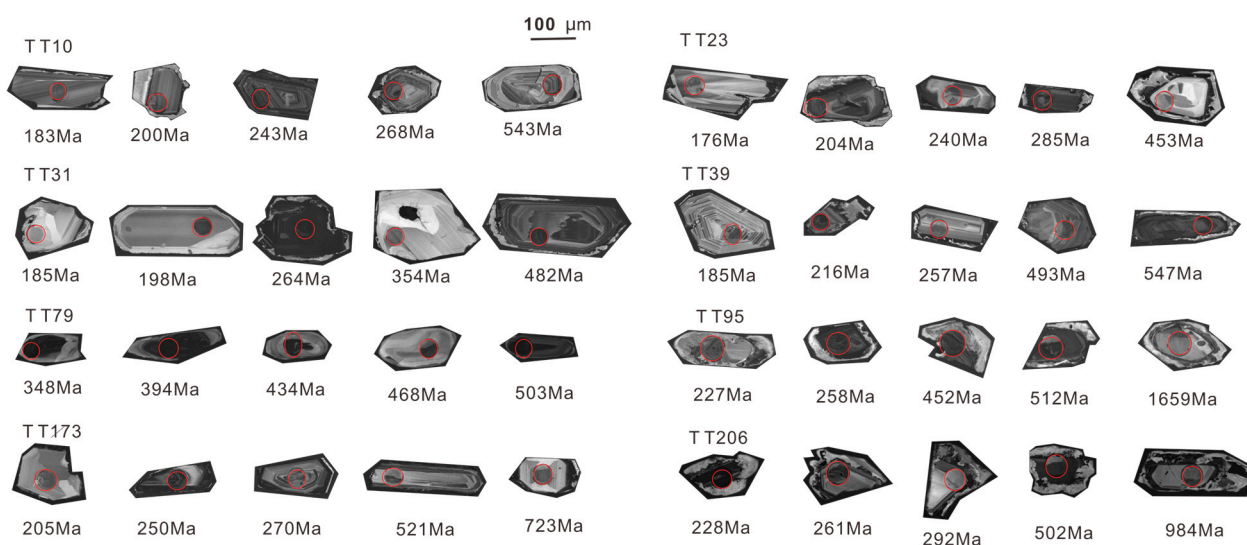


Figure 5. CL images of the analyzed zircons from the 8 meta-sedimentary rocks. Please see the main text for descriptions. Red circles denote the laser spots during the geochronological analyses.

In sample TT31, zircon grains are slightly larger than those from the former two samples, with lengths ranging from 100 to 300 μm (Figure 5). There are 111 concordant ages in sample TT31 (Figure 6c). Three age populations are subdivided from c. 176 to 1474 Ma: 444–486.6 Ma (13.5%), 240.9–272.8 Ma (28.8%), and 176.1–206.1 Ma (27.9%). This sample shows two major peaks at c. 185 and 263 Ma, respectively, with a minor peak at c. 485 Ma. According to the youngest peak age at c. 185 Ma, the maximum depositional age of sample TT10 is the Early Jurassic.

Zircons from sample TT39 show angular shapes and various sizes; their lengths range from 50 to 250 μm (Figure 5). They yield 121 concordant ages, varying from c. 181 to 1785 Ma (Figure 6d), showing three major groups: 443–527 Ma (28.9%), 235.9–284.1 Ma (32.2%), and 181–209 Ma (18.1%). The age spectrum is similar to sample TT31, that is, it has two major peaks at 185 and 257 Ma, respectively, with a weak peak at about 490 Ma. The maximum depositional age of sample TT10 should be the Early Jurassic, according to the youngest peak age at c. 181 Ma.

Zircons from sample TT79 are different from other samples because no low temperature alteration can be recognized. This sample probably experienced higher metamorphic grade because some zircons have metamorphic overgrowth rims (Figure 5). One hundred and seven concordant ages from sample TT79 (Figure 6e) were obtained. They range from 251 to 769 Ma, and thus, sample TT79 is the only one with no Mesozoic age peak in this study. The ages show a quasi-continuous distribution, and the most important age population is 339 to 556 Ma (87%) with a peak age at c. 468 Ma. Although some younger (Permian to Middle Triassic) and older (Proterozoic) ages exist, they are insignificant, indicating that the maximum depositional age of sample TT79 should be in the Early Triassic.

With similar shapes and sizes (lengths from 80 to 200 μm) to other samples (Figure 5), zircons from sample TT95 have wider hydrothermal altered rims and yielded 101 concordant ages, which vary from 221 to 1818 Ma and is subdivided into four groups (Figure 6f): 500–539 Ma (12.7%), 422–461 Ma (8.8%), 236–289.8 Ma (28.4%) and 218–228.6 Ma (10.8%). There are three major peak ages in this sample, 226 Ma, 259 Ma, and 512 Ma. According to the ages of the youngest zircon grain at c. 221 Ma and peak at c. 226 Ma, the maximum depositional age of this sample is the Late Triassic.

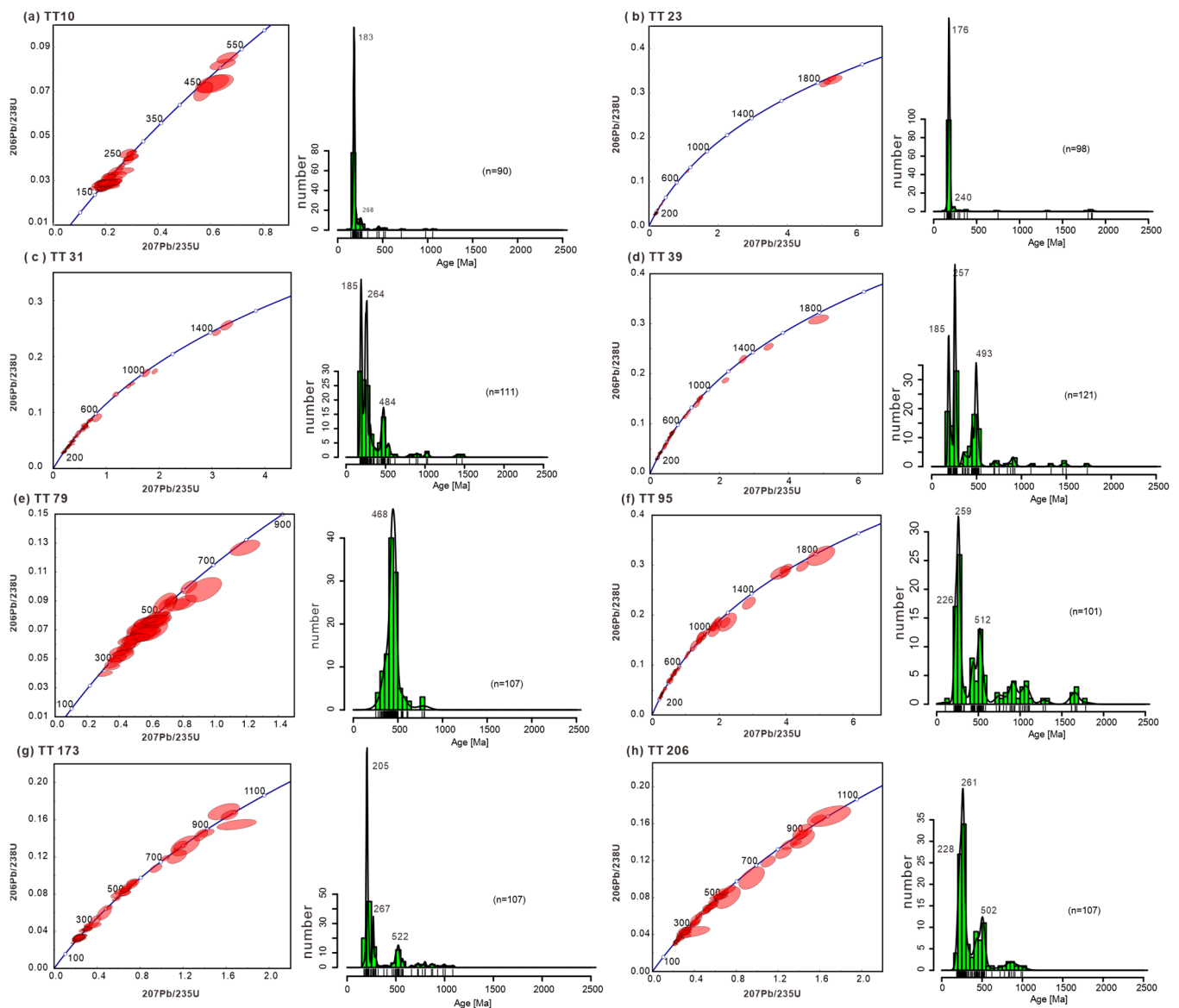


Figure 6. Detrital zircon U-Pb dating results of samples in this study. For each sample, the concordant diagram is shown in the left, and the histogram with a KDE curve is in the right. The figure was illustrated using IsoplotR [31] and refers to [32,33].

The hydrothermal rims of zircons are thin in sample TT173. One hundred and seven grains yielded concordant ages between 177 and 1004 Ma in this sample (Figure 6g), which show three major age populations, 501–537 Ma (10.2%), 250–296 Ma (14.0%) and 177–225 Ma (57.9%) corresponding to three major peak ages at 522, 267, and 205 Ma, respectively. The maximum depositional age of sample TT193 should be the earliest Jurassic, according to the youngest several grains which have ages from 177 to 199 Ma.

The low temperature alteration was remarkable in sample TT206 because of the wide rims with irregular complicated internal structures (Figure 5). We obtained 107 concordant ages from this sample, which range from 185 Ma to 999 Ma (Figure 6h). Three age groups can be recognized in this sample, that is, 829–906 Ma (4.7%), 486–529 Ma (14.0%) and 202–296 Ma (57.0%). Age peak at c. 261 Ma is the most important one relative to the other two at c. 228 Ma and 502 Ma, respectively. Although the youngest age peak is 228 Ma, the maximum depositional age of this sample should be the Early Jurassic, because there are six grains showing ages from 200 to 185 Ma.

4. Discussion

4.1. Types of Detrital Zircon Age Spectra and Provenance Analysis

We recognize three types of age spectra from the 8 meta-sedimentary rock samples in this study. The first one is a unimodal type, including samples TT10 and TT23 (Figure 6). Each of them only contains one major peak having ages of the Early Jurassic, 183 Ma and 176 Ma, respectively. Generally, this kind of age spectrum should be related to the intra-oceanic island arc [34] because oceanic arc-related basins are usually separated from the ancient continents by deep trench, abyssal plain, or middle ocean ridge. These positive/negative topographic anomalies are similar to the communication between oceanic arc-related basins and the old continents. Thus, sediments in these basins are mainly from the juvenile island arc, showing a unimodal peak pattern. However, this is not the case in the Heilongjiang Complex because the zircon grains with ages from Paleozoic to Neoproterozoic cannot be ignored in both samples (TT10 and TT23), indicating that they contain materials not only from the young arc, but also from the old continental basement. The depositional environment is not intra-oceanic arc, but near a continental arc. The second type is trimodal type, showing three major peak ages at the Late Triassic to Early Jurassic, Late Permian to Early Triassic, and Early Paleozoic. The three age peaks of this “trimodal” type can be recognized in the first type (unimodal). However, in the latter type, the Late Triassic to Early Jurassic age group is much more important than any other ages. In the second type, however, the Late Permian to Early Triassic and Early Paleozoic age groups are increasingly significant. The two post-Paleozoic age populations are contrasting. In sample TT173, the Late Triassic to Early Jurassic peak is much higher, but in other cases, the Late Permian to Early Triassic is equally (sample TT31) or even more (samples TT39, TT95, and TT206) important. The third type of age spectrum only contains sample TT79. It is special because the Mesozoic ages are quite fewer in this sample than in all other ones.

The three types of the detrital zircon age spectrum match the magmatic records in the Jiamusi block and the Lesser Xing’an-Zhangguangcai Range, suggesting the source region should be the continental blocks on both sides. For example, the most common age in the Jiamusi block is the Early Paleozoic (c. 530 to 450 Ma), representing the late Pan-African granulite-facies metamorphism and its accompanying or later-stage felsic magmatism [25]. Thus, the third type (sample TT79) probably suggests that it mainly accepted the sediments from the east side, the Jiamusi block, with only very minor materials from the west. Along the western margin of the Jiamusi block, numerous granitic gneisses and weakly deformed granitoids are exposed and show I-type geochemical features. Their ages continuously vary from c. 275 to 245 Ma, with a peak age at 260–250 Ma. This age population is quite common in most samples in this study (samples TT31, TT39, TT95, TT173, and TT206), indicating the important contribution of the western Jiamusi block to the Heilongjiang Complex. However, the Late Triassic to Middle Jurassic (c. 210–170 Ma) magmatism is almost undetectable in the Jiamusi block but occur as the most important ages in the Lesser Xing’an-Zhangguangcai Range [10,22]. Thus, the first and second types of age spectrum should be largely containing materials from this range, namely the eastern Songliao block because age peaks at 170–210 Ma are usually high as or higher than those at 250–260 Ma (Figure 6).

Therefore, our provenance analyses indicate that the Heilongjiang Complex mainly contains deposits of terrigenous materials from both sides, that is, the Jiamusi and Songliao blocks. Although all these samples were collected from the Heilongjiang Complex, the relative contributions of the two blocks differ. Some samples (the first type) mainly consisted of materials from the west side, for example, the samples TT10 and TT23; other samples (the second type) accepted materials from both sides, including samples TT31, TT39, TT95, TT173, and TT206; the sediments of only one sample (TT79, the third type) was mainly supplied by the Jiamusi Block. The provenance complexity of the Heilongjiang Complex is consistent with the nature of the “non-Smith strata” of the accretionary complex. Accretionary complexes are formed after the closure of fossil oceanic basins and thus near the suture zones. They show a complicated “block-in-matrix” structure. Although they are mainly composed of meta-sedimentary rocks, the original sequence has been disturbed.

Rocks that have quite different provenance and metamorphic history are stacked together after the emplacement of the accretionary complex.

4.2. Two Crustal Thickening Events in NE China Revealed by Zircon and Whole-Rock Geochemistry

The provenance analysis result—the detrital zircons in this study are mainly derived from the Songliao and Jiamusi blocks—indicates that the zircon trace elements can reflect the geochemical variations of their sources [16], the regional magmatic rocks. This provides a basis to our following discussions on magmatic and tectonic evolution.

Zircon trace elements are strongly controlled by the magma compositions from which they crystallize, which further record the temperature and pressure conditions influenced by tectonics. For example, zircon Eu anomaly ($\text{Eu}_N/\sqrt{\text{Gd}_N \times \text{Sm}_N}$; the subscript N means normalized to chondrites) [35] is used together with the whole-rock Sr/Y and La/Yb ratios [36] of felsic magmatic rocks to discuss the crustal thickness. The hypothesis is that crustal magmas are usually formed either by differentiation or crustal partial melting [37]. Both processes tend to occur at depths where mantle-derived stall, such as Moho. During the formation of these crustal magmas, the stability fields of some minerals are mainly associated with pressure, such as garnet (rich in HREEs and Y), plagioclase (rich in Sr and Eu^{2+}), and amphibole (rich in middle to heavy REEs). Under higher pressure, amphibole and garnet tend to crystallize and plagioclase will break down. Thus, higher/lower whole-rock Sr/Y and La/Yb ratios indicate higher/lower pressure of felsic magmas, or deeper/shallower Moho depth [16]. Instable plagioclase under high pressure will release more Eu into the magma and increase the magmatic Eu anomaly, which will finally produce zircons with higher Eu anomaly values than those formed under lower pressure [35]. Accordingly, we will discuss the variation of magmatic formation depth by employing these geochemical proxies, based on both our new detrital zircon data and previously published data. Using the compiled geochronological and geochemical data from the regional magmatic rocks, we discuss the tectonic evolution of this region and its implications for the continental flare-ups along the active continental margin.

Detrital zircon trace elements reveal two crustal thickening events (Figure 7A–C), which coeval with the regional magmatic flare-up events: the first one lasted from the Early Permian to Early Triassic and the second mainly occurred in the Early Jurassic (Figure 7F). The median value of Eu/Eu* increased from <0.2 at c. 280 Ma to 0.5 at c. 245 Ma (Figure 7A) and decreased back to 0.2 in the Middle Triassic. Afterwards, the median value of Eu/Eu* again increased slowly to 0.4 at c. 180 Ma. This increase indicates that the crust was probably thickened during the two episodes of magmatic flare-ups, leading to the breakdown of plagioclase in the source and the higher zircon Eu/Eu* values in the magmas. During the magmatic lull from the Middle to Late Triassic, the crust thinned, facilitating the stabilization of plagioclase in the source region.

Similar to the Eu/Eu* values, the $(\text{Dy}/\text{Yb})_N$ values in the detrital zircons are also low during the magmatic lull but higher in the flare-ups (Figure 7b). The median of the $(\text{Dy}/\text{Yb})_N$ values fluctuated around 0.2 in the Permian and slightly increased from 0.17 to 0.2 in the Late Triassic to Early Jurassic. In the Middle to Late Triassic, it decreased to near 0.15. This means that the middle REEs were depleted relative to the heavy REEs in the magmatic lull, indicating that stabilization of amphiboles weakened and thus the crustal probably thinned.

Zircon Th/U ratio is commonly used to distinguish the magmatic or metamorphic origins of zircons [38], with the former being usually higher than 0.1 and the later being lower. In this study, almost all the zircons (<290 Ma) have Th/U ratios > 0.1, indicating their magmatic origins and thus the temporal change of this value should not be related to any metamorphic processes. In the intermediate to felsic magmas, monazite and allanite are common accessory minerals controlling the Th and U budgets. Specially, Th is more compatible in these minerals than U and thus their fractionation will lead to low Th/U ratio in other minerals. Some studies indicate that the early-stage crystallization of Th-rich

minerals relative to zircon occurs in low-temperature magmas, whereas these minerals are unstable in high-temperature magmas [39]. Thus, high Th/U ratio probably indicates high magmatic temperature. During the crustal thickening event, the deep crust becomes warmer when the geothermal gradient remains constant; a thicker crust is able to keep the magma reservoir warm, accelerating the Th/U ratios, similar to the examples in the Cretaceous Sikhote-Alin arc magmas [40] and Mesozoic Andes [16,41]. In this study, higher Th/U ratio corresponds to higher zircon Eu/Eu*, whole-rock Sr/Y, and $(La/Yb)_N$, probably representing the crustal thickening events. The low zircon Th/U ratios during the Middle to Late Triassic may have resulted from the crustal magmas produced in shallower crust and thus in lower temperatures.

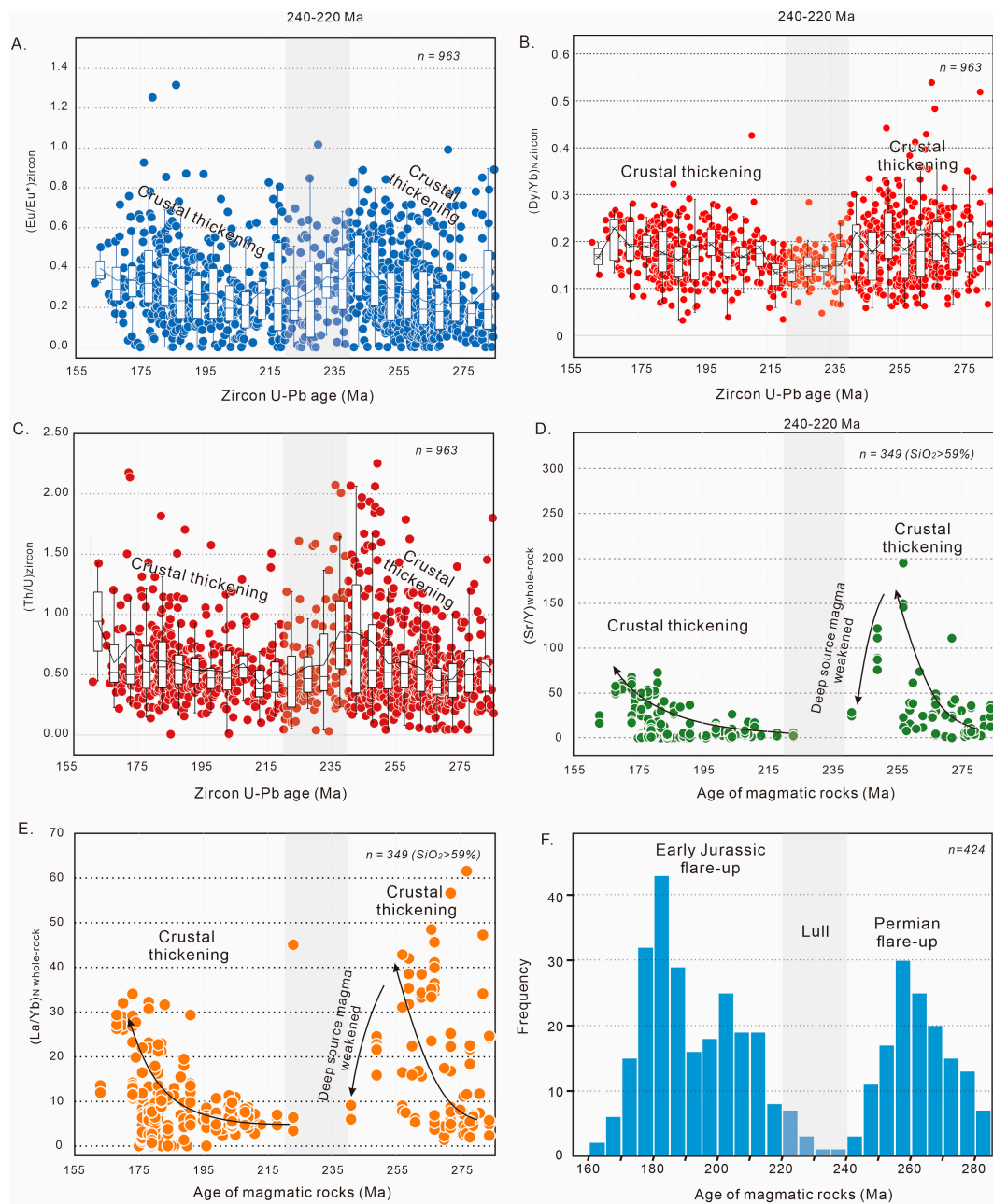


Figure 7. Trace elements geochemical data (shown in different colors) from the regional magmatic rocks and detrital zircons in this study. Part of the detrital zircon data are from [13]. (A–C) show Eu anomaly, Th/U and Dy/Yb ratios of zircons varying with zircon ages, respectively; (D,E) show whole-rock Sr/Y and $(La/Yb)_N$ ratios varying with rock ages, respectively; (F) age histogram of magmatic rocks (Permian to Jurassic).

Whole-rock trace elements of the compiled magmatic rocks show consistent trends with the zircon Eu/Eu^* , $(\text{Dy}/\text{Yb})_N$ and Th/U ratios. Two crustal thickening events are revealed by high Sr/Y and $(\text{La}/\text{Yb})_N$ ratios (Figure 7D,E). The first occurred in the Permian, during which the whole-rock Sr/Y ratios increased from 10–40 to >150, and the $(\text{La}/\text{Yb})_N$ ratios also increased from <10 to >40. The second lasted from the Late Triassic to Early Jurassic when the Sr/Y ratios increased from <10 to >50, whereas the $(\text{La}/\text{Yb})_N$ ratios increased from about 5 to 35. The good coherence between the two ratios indicates that the source of these felsic magmatic rocks changed from low pressure to high, indicating that the crust was possibly thickened at that time [42]. It should be noted that during the Middle to Late Triassic, both ratios decreased remarkably, suggesting that the deep magma source (high pressure) was shut down and only the shallow-level (low pressure) magmas were active.

In a word, trace elements of both the whole rock and detrital zircon reveal two events of crustal thickening in NE China during the Permian and Early Jurassic, respectively. Each thickening event was coeval with a continental flare-up (Figure 7F). Between them, the volume of deep source magmas reduced with the shallow ones remaining active, accompanied by an important magmatic lull (Figure 7F).

4.3. Tectono-Magmatic Evolution in NE China: Not a “Cyclic Orogen”

The tectono-magmatic evolution in NE China shares similarities with the proposed “cyclic orogen”, such as in the American Cordillera [3]. The most important fact is that crustal thickening was accompanied by continental arc flare-ups and landward arc migration (Figure 8). During the Permian flare-up, the arc-related andesite and other volcanic rocks in the Erlongshan Formation was distributed along the eastern margin of the Jiamusi block in the Early Permian. At the end of the Permian, most magmatism had migrated to the Yilan-Mudanjiang alignment and the migrating distance was about 180 km (Figure 8A). During the Late Triassic to Middle Jurassic, the magmatic rocks migrated westwards from Hegang-Yilan-Mudanjiang to Tieli-Jilin, and the distance approximated to 150 km (Figure 8B).

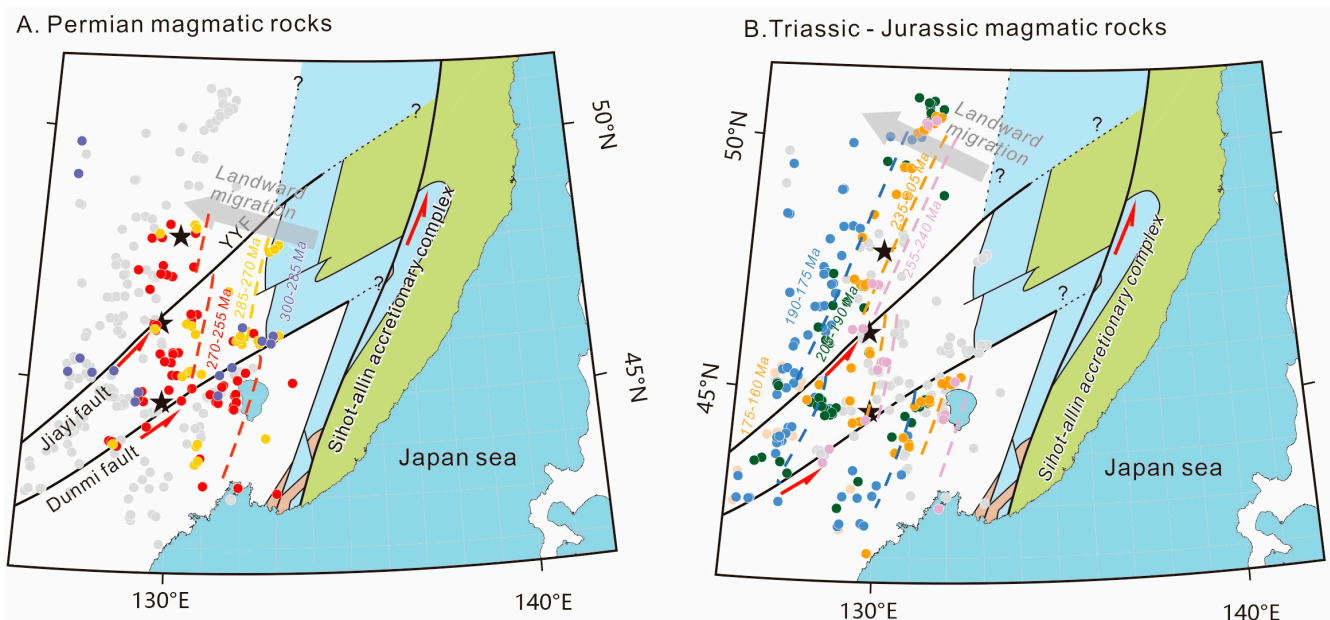


Figure 8. Spatial distribution of regional magmatic rocks. (A,B) show the westward younger trends of the Permian and Triassic-Jurassic calc-alkaline magmatic rocks (continental arc), respectively. Black stars show the positions of Luobei, Yilan, and Mudanjiang from north to south. The supposed extensions of the major faults are shown by dashed lines with question marks.

However, there are significant differences between the cases in NE China and the American Cordillera. The first is the nature of the arc magmatic migration. In NE China, the two migrations were independent from each other, that is, during the magmatic lull the magmas did not move back to the trench (east) but consistently migrated landward (westward) (Figure 8). However, in the American Cordillera, continental arc fronts tended to migrate towards the trench during the lulls and moved landwards again when the magmatic flare-ups were onset [3,5]. This difference indicates that the twice orogenic events in NE China, marked by the two magmatic flare-ups and crustal thickening events, were not two orogenic episodes within a single “cyclic orogen”. The second difference is that regional extension was active in NE China during the orogenic events, evident from the opening of the Mudanjiang Ocean and regional A-type and bimodal volcanism [10]. In the Heilongjiang Complex, metamorphic oceanic crustal fragments were preserved as exhumed blocks within the strongly deformed matrix, such as MORB and OIB-like blueschist and greenschist, representing the opening of the Mudanjiang Ocean and island arc within it [15]. The protolith ages of these remnants of the oceanic crust range from c. 210 Ma to 290 Ma. In the Late Triassic, A-type and bimodal volcanic rocks were reported in the Lesser Xing’an-Zhangguangcai Range and Khanka block [10], indicating the occurrence of intra-continental extension during that period.

4.4. Tectonic Implications in NE China: Two Orogenic Events during the Closure of the Mudanjiang Ocean

According to the similarities and differences between magmatism in NE China and the American Cordillera, we propose a new model in our study area in order to explain the coupling between magmatic flare-up, landward migration, and crustal thickening (Figure 9).

During the early Permian, the eastern Jiamusi margin experienced a transition from a passive continental margin to an active one [26]. This transition produced a series of arc-related volcanic rocks with sedimentary strata (Figure 9A), aligning from north to south near Baoqing. Since then, the oceanic plate within the Panthalassa Ocean began to subduct beneath the Jiamusi block and triggered the first orogenic event in NE China. The slab dip angle became shallower as the oceanic plate subducted and thus resulted in the landward migration of the calc-alkaline magmatism in the Jiamusi block. The coupling between the overriding and subducting plates was strengthened, and thus the crust was thickened (Figure 9B). Crustal thickening caused warmer lower crust and deeper Moho in the region, facilitating deep crustal melting and resulted in more voluminous magmas in the Permian, namely the first magmatic flare-up. However, the asthenospheric mantle wedge could be largely expelled by the shallowing slab and thickening arc crust, and thus the arc magmatic source weakened after it migrated to the western margin of the Jiamusi block (Figure 9C). Deep source melting also vanished, causing the descending trend in the whole-rock Sr/Y, (La/Yb)_N, and zircon Eu/Eu*, Th/U, and (Dy/Yb)_N ratios.

From the Early Triassic, the Mudanjiang Oceanic plate probably began to subduct westwards and produced calc-alkaline magmatism in the Lesser Xing’an-Zhangguangcai Range, the second continental arc flare-up (Figure 9D). Magmatism also moved westwards during the Middle Triassic to Middle Jurassic, probably related to the shallowing subducting slab dip, or associated with the removal of the fore-arc crust by subduction erosion. Regional extension may have existed in the arc or back-arc region during the Middle-Late Triassic, making the regional tectonics complicated than our schematic tectonic model. The closure of the Mudanjiang Ocean occurred after the Early Jurassic (the maximum depositional ages of most samples in this study), which should be the reason why the Early Jurassic magmatic flare-up ended abruptly at c. 170 Ma (Figure 9E) without remarkable decrease in the values of the whole-rock Sr/Y, (La/Yb)_N, and zircon Eu/Eu* ratios.

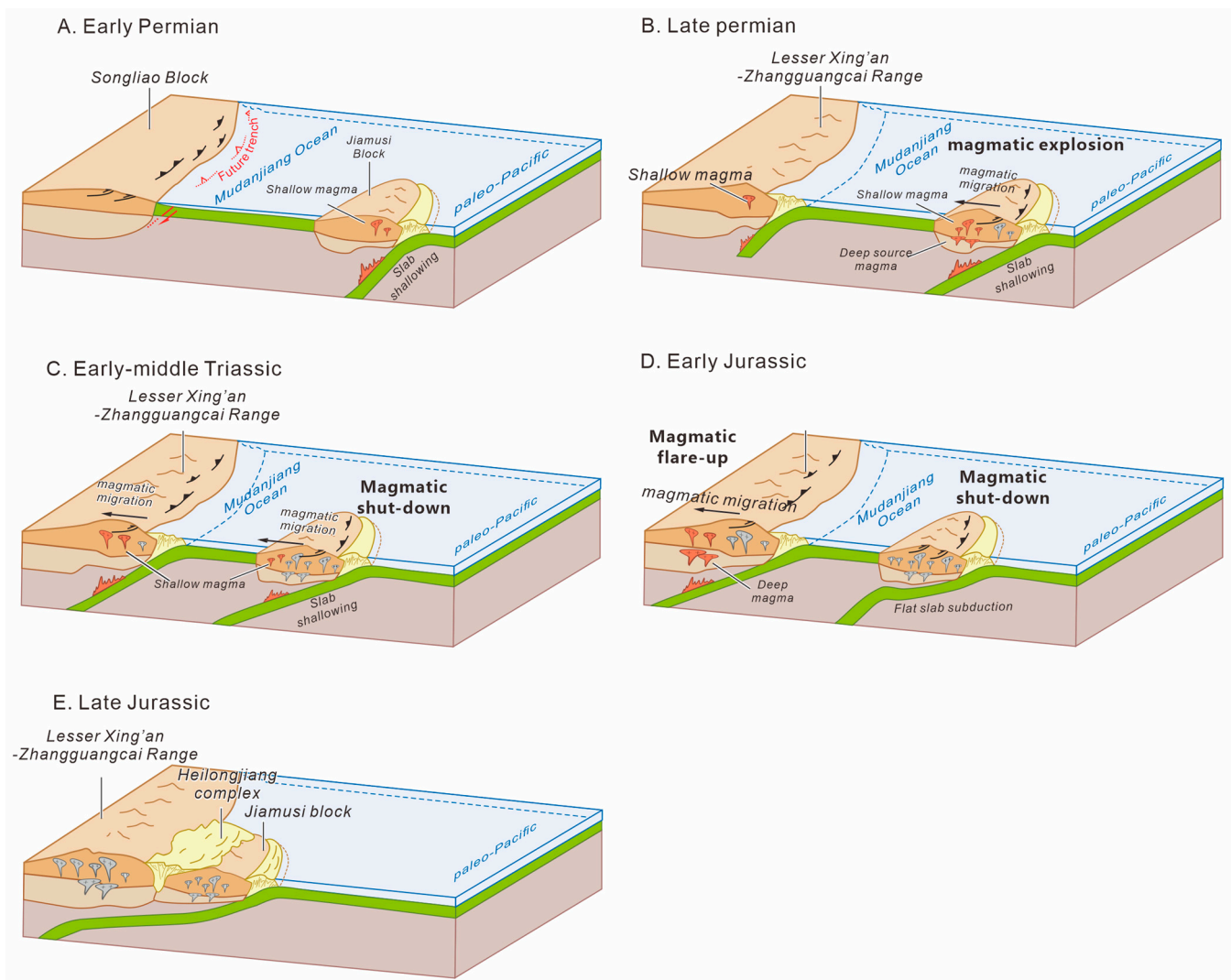


Figure 9. Tectono-magmatic evolution in the eastern Heilongjiang Province. It illustrates the two episodes of continental arc magmatic flare-ups and crustal thickening history.

5. Conclusions

The Heilongjiang Complex mainly received sediments from the both sides, including the Songliao block (the Lesser Xing'an-Zhangguangcai Range) and Jiamusi block, recording abundant geochemical information of the Permian to Middle Jurassic magmatism in NE China.

Trace elements from the detrital zircons (Eu/Eu^* , Th/U , and $(Dy/Yb)_N$ ratios) and regional magmatic rocks (whole-rock Sr/Y , $(La/Yb)_N$) both indicate two crustal thickening events in the Permian and Early Jurassic, respectively. Crustal thickening was accompanied by magmatic flare-up and landward migration.

The two crustal thickening events and flare-ups are independent of each other, forming two orogenic events in NE China. The Permian crustal thickening event was caused by shallowing subducting slab angle and thus triggered magmatic flare-ups. The shallow slab subduction enhanced plate coupling and caused the westward subduction of the Mudanjiang Oceanic plate, generating the second flare-up in this region and the crustal thickening event.

Closure of the back-arc basin or marginal sea (the Mudanjiang Ocean) by the subduction of the Paleo-Pacific oceanic plate (Izanagi plate) could lead to several arc magmatic flare-ups and crustal thickening events, as revealed by our study. This is probably a com-

mon process in the accretionary orogens and contributed to the continental growth along active continental margins.

Supplementary Materials: The following supporting information can be downloaded at: <https://www.mdpi.com/article/10.3390/min13091121/s1>, Table S1. Detrital zircon U-Pb dating and trace elements results; Table S2. Data for Figure 7d,e; Table S3. Analytical methods. References [43,44] are cited in the Supplementary Materials.

Author Contributions: Conceptualization, K.L. and M.X.; methodology, K.L. and Y.P.; software, K.L. and Y.P.; validation, K.L. and Y.P.; formal analysis, M.X.; investigation, K.L., M.W. and Y.P.; resources, K.L.; data curation, K.L. and Y.P.; writing—original draft preparation, K.L. and Y.P.; writing—review and editing, K.L.; visualization, K.L. and Y.P.; supervision, K.L. and M.W.; project administration, K.L.; funding acquisition, K.L. All authors have read and agreed to the published version of the manuscript.

Funding: This research was funded by the National Natural Science Foundation of China (42272252, 41902233).

Data Availability Statement: The authors confirm that the data generated or analyzed during this study are provided in full within the published article. Zircon U-Pb and trace elements data from reference [13] are also compiled to generate the figures.

Acknowledgments: We deeply appreciate the discussions with Wenliang Xu and Jianbo Zhou on the tectonics in NE China.

Conflicts of Interest: The authors declare no conflict of interest.

References

1. Chapman, J.B.; Shields, J.E.; Ducea, M.N.; Paterson, S.R.; Attia, S.; Ardill, K.E. The causes of continental arc flare ups and drivers of episodic magmatic activity in Cordilleran orogenic systems. *Lithos* **2021**, *398–399*, 106307. [CrossRef]
2. Paterson, S.R.; Ducea, M.N. Arc Magmatic Tempos: Gathering the Evidence. *Elements* **2015**, *11*, 91–98. [CrossRef]
3. DeCelles, P.G.; Ducea, M.N.; Kapp, P.; Zandt, G. Cyclicity in Cordilleran orogenic systems. *Nat. Geosci.* **2009**, *2*, 251–257. [CrossRef]
4. Lee, C.-T.A.; Thurner, S.; Paterson, S.; Cao, W. The rise and fall of continental arcs: Interplays between magmatism, uplift, weathering, and climate. *Earth Planet. Sci. Lett.* **2015**, *425*, 105–119. [CrossRef]
5. Ducea, M. The California Arc: Thick Granitic Batholiths, Eclogitic Residues, Lithospheric-Scale Thrusting, and Magmatic Flare-Ups. *GSA Today* **2001**, *11*, 4. [CrossRef]
6. Chapman, A.D.; Saleeby, J.B.; Eiler, J. Slab Fattening Trigger for Isotopic Disturbance and Magmatic Flare-up in the Southernmost Sierra Nevada Batholith, California. *Geology* **2013**, *41*, 1007–1010. [CrossRef]
7. Karlstrom, L.; Lee, C.-T.A.; Manga, M. The role of magmatically driven lithospheric thickening on arc front migration. *Geochem. Geophys. Geosystems* **2014**, *15*, 2655–2675. [CrossRef]
8. Chapman, J.B.; Ducea, M.N. The role of arc migration in Cordilleran orogenic cyclicity. *Geology* **2019**, *47*, 627–631. [CrossRef]
9. Attia, S.; Cottle, J.M.; Paterson, S.R. Erupted zircon record of continental crust formation during mantle driven arc flare-ups. *Geology* **2020**, *48*, 446–451. [CrossRef]
10. Xu, W.-L.; Pei, F.-P.; Wang, F.; Meng, E.; Ji, W.-Q.; Yang, D.-B.; Wang, W. Spatial-temporal relationships of Mesozoic volcanic rocks in NE China: Constraints on tectonic overprinting and transformations between multiple tectonic regimes. *J. Asian Earth Sci.* **2013**, *74*, 167–193. [CrossRef]
11. Yang, H.; Ge, W.; Dong, Y.; Bi, J.; Wang, Z.; Ji, Z. Record of Permian–Early Triassic continental arc magmatism in the western margin of the Jiamusi Block, NE China: Petrogenesis and implications for Paleo-Pacific subduction. *Int. J. Earth Sci.* **2016**, *106*, 1919–1942. [CrossRef]
12. Sun, M.; Chen, H.; Milan, L.A.; Wilde, S.A.; Jourdan, F.; Xu, Y. Continental Arc and Back-Arc Migration in Eastern NE China: New Constraints on Cretaceous Paleo-Pacific Subduction and Rollback. *Tectonics* **2018**, *37*, 3893–3915. [CrossRef]
13. Dong, Y.; Ge, W.-C.; Yang, H.; Ji, Z.; He, Y.; Zhao, D.; Xu, W. Convergence history of the Jiamusi and Songnen-Zhangguangcai Range massifs: Insights from detrital zircon U-Pb geochronology of the Yilan Heilongjiang Complex, NE China. *Gondwana Res.* **2018**, *56*, 51–68. [CrossRef]
14. Liu, K.; Wilde, S.A.; Zhang, J.; Xiao, W.; Wang, M.; Ge, M. Zircon U-Pb dating and whole-rock geochemistry of volcanic rocks in eastern Heilongjiang Province, NE China: Implications for the tectonic evolution of the Mudanjiang and Paleo-Pacific oceans from the Jurassic to Cretaceous. *Geol. J.* **2019**, *55*, 1866–1889. [CrossRef]

15. Zhou, J.-B.; Wilde, S.A.; Zhang, X.-Z.; Zhao, G.-C.; Zheng, C.-Q.; Wang, Y.-J.; Zhang, X.-H. The onset of Pacific margin accretion in NE China: Evidence from the Heilongjiang high-pressure metamorphic belt. *Tectonophysics* **2009**, *478*, 230–246. [[CrossRef](#)]
16. Sundell, K.E.; George, S.W.; Carrapa, B.; Gehrels, G.E.; Ducea, M.N.; Saylor, J.E.; Pepper, M. Crustal Thickening of the Northern Central Andean Plateau Inferred from Trace Elements in Zircon. *Geophys. Res. Lett.* **2022**, *49*, e2021GL096443. [[CrossRef](#)]
17. Wilde, S.A. Final amalgamation of the Central Asian Orogenic Belt in NE China: Paleo-Asian Ocean closure versus Paleo-Pacific plate subduction—A review of the evidence. *Tectonophysics* **2015**, *662*, 345–362. [[CrossRef](#)]
18. Pei, F.; Xu, W.; Yang, D.; Zhao, Q.; Liu, X.; Hu, Z. Zircon U-Pb geochronology of basement metamorphic rocks in the Songliao Basin. *Chin. Sci. Bull.* **2007**, *52*, 942–948. [[CrossRef](#)]
19. Song, Y.; Stepashko, A.; Liu, K.; He, Q.; Shen, C.; Shi, B.; Ren, J. Post-rift Tectonic History of the Songliao Basin, NE China: Cooling Events and Post-rift Unconformities Driven by Orogenic Pulses from Plate Boundaries. *J. Geophys. Res. Solid Earth* **2018**, *123*, 2363–2395. [[CrossRef](#)]
20. Song, Y.; Ren, J.; Liu, K.; Lyu, D.; Feng, X.; Liu, Y.; Stepashko, A. Syn-rift to post-rift tectonic transition and drainage reorganization in continental rifting basins: Detrital zircon analysis from the Songliao Basin, NE China. *Geosci. Front.* **2022**, *13*, 101377. [[CrossRef](#)]
21. Wang, P.-J.; Mattern, F.; Didenko, N.A.; Zhu, D.-F.; Singer, B.; Sun, X.-M. Tectonics and cycle system of the Cretaceous Songliao Basin: An inverted active continental margin basin. *Earth-Sci. Rev.* **2016**, *159*, 82–102. [[CrossRef](#)]
22. Wu, F.Y.; Sun, D.Y.; Ge, W.C.; Zhang, Y.B.; Grant, M.L.; Wilde, S.A.; Jahn, B.M. Geochronology of the Phanerozoic granitoids in northeastern China. *J. Asian Earth Sci.* **2011**, *41*, 1–30. [[CrossRef](#)]
23. Yang, H.; Ge, W.-C.; Zhao, G.-C.; Bi, J.-H.; Wang, Z.-H.; Dong, Y.; Xu, W.-L. Zircon U–Pb ages and geochemistry of newly discovered Neoproterozoic orthogneisses in the Mishan region, NE China: Constraints on the high-grade metamorphism and tectonic affinity of the Jiamusi–Khanka Block. *Lithos* **2017**, *268–271*, 16–31. [[CrossRef](#)]
24. Sorokin, A.A.; Ovchinnikov, R.O.; Kudryashov, N.M.; Sorokina, A.P. An Early Neoproterozoic gabbro–granite association in the Bureya Continental Massif (Central Asian fold belt): First geochemical and geochronological data. *Dokl. Earth Sci.* **2016**, *471*, 1307–1311. [[CrossRef](#)]
25. Zhou, J.-B.; Wilde, S.A.; Zhang, X.-Z.; Zhao, G.-C.; Liu, F.-L.; Qiao, D.-W.; Ren, S.-M.; Liu, J.-H. A > 1300 km late Pan-African metamorphic belt in NE China: New evidence from the Xing’an block and its tectonic implications. *Tectonophysics* **2011**, *509*, 280–292. [[CrossRef](#)]
26. Li, G.-Y.; Zhou, J.-B.; Li, L. The Jiamusi Block: A hinge of the tectonic transition from the Paleo-Asian Ocean to the Paleo-Pacific Ocean regimes. *Earth-Sci. Rev.* **2022**, *236*, 104279. [[CrossRef](#)]
27. Liu, K.; Zhang, J.; Wilde, S.A.; Zhou, J.; Wang, M.; Ge, M.; Wang, J.; Ling, Y. Initial subduction of the Paleo-Pacific Oceanic plate in NE China: Constraints from whole-rock geochemistry and zircon U–Pb and Lu–Hf isotopes of the Khanka Lake granitoids. *Lithos* **2017**, *274–275*, 254–270. [[CrossRef](#)]
28. Zhu, C.Y.; Zhao, G.; Sun, M.; Liu, Q.; Han, Y.; Hou, W.; Zhang, X.; Eizenhofer, P.R. Geochronology and geochemistry of the Yilan blueschists in the Heilongjiang Complex, northeastern China and tectonic implications. *Lithos* **2015**, *216–217*, 241–253. [[CrossRef](#)]
29. Wang, F.; Xu, W.-L.; Gao, F.-H.; Meng, E.; Cao, H.-H.; Zhao, L.; Yang, Y. Tectonic history of the Zhangguangcailing Group in eastern Heilongjiang Province, NE China: Constraints from U–Pb geochronology of detrital and magmatic zircons. *Tectonophysics* **2012**, *566–567*, 105–122. [[CrossRef](#)]
30. Rubatto, D. Zircon: The Metamorphic Mineral. *Rev. Mineral. Geochem.* **2017**, *83*, 261–295. [[CrossRef](#)]
31. Vermeesch, P. IsoplotR: A free and open toolbox for geochronology. *Geosci. Front.* **2018**, *9*, 1479–1493. [[CrossRef](#)]
32. Fornelli, A.; Micheletti, F.; Langone, A.; Perrone, V. First U–Pb detrital zircon ages from Numidian sandstones in Southern Apennines (Italy): Evidences of African provenance. *Sediment. Geol.* **2015**, *320*, 19–29. [[CrossRef](#)]
33. Fornelli, A.; Micheletti, F.; Gallicchio, S.; Tursi, F.; Criniti, S.; Critelli, S. Detrital zircon ages of Oligocene to Miocene sandstone suites of the Southern Apennines foreland basin system, Italy. *J. Palaeogeogr.* **2022**, *11*, 222–237. [[CrossRef](#)]
34. Cawood, P.; Hawkesworth, C.; Dhuime, B. Detrital zircon record and tectonic setting. *Geology* **2012**, *40*, 875–878. [[CrossRef](#)]
35. Tang, M.; Ji, W.-Q.; Chu, X.; Wu, A.; Chen, C. Reconstructing crustal thickness evolution from europium anomalies in detrital zircons. *Geology* **2020**, *49*, 76–80. [[CrossRef](#)]
36. Profeta, L.; Ducea, M.N.; Chapman, J.B.; Paterson, S.R.; Gonzales, S.M.H.; Kirsch, M.; Petrescu, L.; DeCelles, P.G. Quantifying crustal thickness over time in magmatic arcs. *Sci. Rep.* **2015**, *5*, 17786. [[CrossRef](#)]
37. Farner, M.J.; Lee, C.-T.A. Effects of crustal thickness on magmatic differentiation in subduction zone volcanism: A global study. *Earth Planet. Sci. Lett.* **2017**, *470*, 96–107. [[CrossRef](#)]
38. Yakymchuk, C.; Kirkland, C.L.; Clark, C. Th/U ratios in metamorphic zircon. *J. Metamorph. Geol.* **2018**, *36*, 715–737. [[CrossRef](#)]
39. Harrison, T.M.; Watson, E.B.; Aikman, A.B. Temperature spectra of zircon crystallization in plutonic rocks. *Geology* **2007**, *35*, 635. [[CrossRef](#)]
40. Wu, J.T.-J.; Wu, J.; Alexandrov, I.; Lapen, T.; Lee, H.-Y.; Ivin, V. Continental growth during migrating arc magmatism and terrane accretion at Sikhote-Alin (Russian Far East) and adjacent northeast Asia. *Lithos* **2022**, *432–433*, 106891. [[CrossRef](#)]
41. Jara, J.J.; Barra, F.; Reich, M.; Leisen, M.; Romero, R.; Morata, D. Episodic construction of the early Andean Cordillera unravelled by zircon petrochronology. *Nat. Commun.* **2021**, *12*, 4930. [[CrossRef](#)] [[PubMed](#)]
42. Lieu, W.K.; Stern, R.J. The robustness of Sr/Y and La/Yb as proxies for crust thickness in modern arcs. *Geosphere* **2019**, *15*, 621–641. [[CrossRef](#)]

43. Ji, W.-Q.; Wu, F.-Y.; Wang, J.-M.; Liu, X.-C.; Liu, Z.-C.; Zhang, Z.; Cao, W.; Wang, J.-G.; Zhang, C. Early Evolution of Himalayan Orogenic Belt and Generation of Middle Eocene Magmatism: Constraint From Haweng Granodiorite Porphyry in the Tethyan Himalaya. *Front. Earth Sci.* **2020**, *8*, 236. [[CrossRef](#)]
44. Paton, C.; Hellstrom, J.; Paul, B.; Woodhead, J.; Hergt, J. Iolite: Freeware for the Visualisation and Processing of Mass Spectrometric Data. *J. Anal. At. Spectrom.* **2011**, *26*, 2508–2518. [[CrossRef](#)]

Disclaimer/Publisher’s Note: The statements, opinions and data contained in all publications are solely those of the individual author(s) and contributor(s) and not of MDPI and/or the editor(s). MDPI and/or the editor(s) disclaim responsibility for any injury to people or property resulting from any ideas, methods, instructions or products referred to in the content.